

# Heat Transfer Coefficients on Cakes Baked in a Tunnel Type Industrial Oven

O.D. Baik, S. Grabowski, M. Trigui, M. Marcotte, and F. Castaigne

## ABSTRACT

Using an h-monitor, surface heat flux and effective surface heat transfer coefficients were evaluated during baking of two cakes in a tunnel-type multi-zone industrial oven. An average 75–80% of total heat flux was counted as radiation heat. Air-mass temperature outside the boundary layer was determined from the experimental temperature profiles over the h-monitor top plate. In the range of baking temperatures (186–225°C), relative air velocities (0.02–0.437 m/s) and absolute humidities (0.0267–0.0428 kg H<sub>2</sub>O/kg dry air) heat transfer coefficients were 20 to 48.0 W/m<sup>2</sup>K. A simple regression model was developed based on experimental data.

**Key Words:** cake baking, tunnel-type oven, heat flux, heat transfer, boundary layer

## INTRODUCTION

THE QUALITY OF THE FINAL PRODUCT AND ENERGY DEMAND FOR baking depend mainly on the ingredients used and the procedure applied (Sluimer and Krist-Spit, 1987; Booth, 1990). In general, energy consumption in baking depends on the construction and size of the oven and on operating conditions such as the velocity, temperature and humidity of the hot air. In addition, the thermal properties of cake (from batter to final product) should be known to estimate the energy balance during baking (Baik et al., 1999). A major problem in estimation of the energy consumption in baking is the lack of actual values of heat transfer coefficients.

The direct-fired tunnel oven is the most common type for commercial cake baking. However, heat transfer in such ovens is still unexplored. In particular, a non-uniform temperature distribution between heating elements and product surface is an important factor as well as variable temperature profiles along the continuous oven which makes it difficult to estimate surface heat transfer coefficients.

Some experimental and theoretical studies have been reported to characterize heat transfer coefficients between the dough and the internal oven environment. In most such studies, the heat flux or heat transfer coefficient was measured directly in the oven using a heat flux sensor (typically a metal cylinder or sphere) or commercially available h-monitor (Krist-Spit and Sluimer, 1987; Huang and Mittal, 1995; Sato et al., 1995; Li and Walker, 1996). A direct measurement of the heat transfer coefficient in the oven during the baking process is based on the assumption that heat transfer between the oven and dough is the same as between the oven and the model food (heat flux sensor), usually an aluminum piece fitted with a number of thermocouples.

The heat transfer coefficient must be known for mathematical simulation of heat and moisture transport in baking (Sablani et al., 1998). In typical numerical solutions for calculation of temperature and humidity profiles in a dough sample, the heat transfer coefficient has

been assumed to be constant for the entire baking process (Savoye et al., 1992; Fahloul et al., 1994; Özilgen and Heil, 1994; Zaroni et al., 1994). These have been mainly taken from published data. Most heat flux related work has been reported on bread and biscuit baking. Direct measurement was achieved mostly in ovens constructed for research purposes. In the case of cake baking, Li and Walker (1996) estimated apparent convective heat transfer coefficients using an h-monitor in commercial conveyor ovens. They reported average values during the baking process. Little information has been reported on data and measurement techniques for heat transfer coefficients during cake baking in a tunnel type multi-zone direct fired oven.

The objective of the present study was to determine and analyze the effective surface heat transfer coefficients during cake baking in a tunnel type multi-zone industrial oven.

## MATERIALS & METHODS

### Ovens

**Tunnel type industrial oven.** A tunnel type multi-zone industrial oven was tested for heat transfer coefficient (Fig. 1). The total oven length was 27.97 m; its heating source was electricity, and its heating mode was direct firing. Molds were used as cake batter containers. The oven consisted of four zones with one upper and one lower chamber. Each zone temperature was controlled separately. An endless conveyor belt made of metal rods spaced 12 cm apart allowed continuous baking. Molds loaded with batter passed through the baking chambers with the band moving at a constant speed. Baked cakes were unloaded at the exit. Combustion products and accumulated water vapor were evacuated through the chimney ventilators. Baking time for cake A (process A) was 8 min 36 s, while for cake B (process B) 6 min 27 s. The h-monitor (described later) was kept on the conveyor belt, and the top plate was exposed directly to the hot air. The oven had three inspection holes through the oven walls to test dew point and air velocity. Special adaptors were placed on each inspection hole to avoid any effect on baking during collection of data. There was no access to the baking chamber from outside except these three small inspection holes, the entrance and the exit. Thus, it was not possible to measure wall temperature at different positions along the oven.

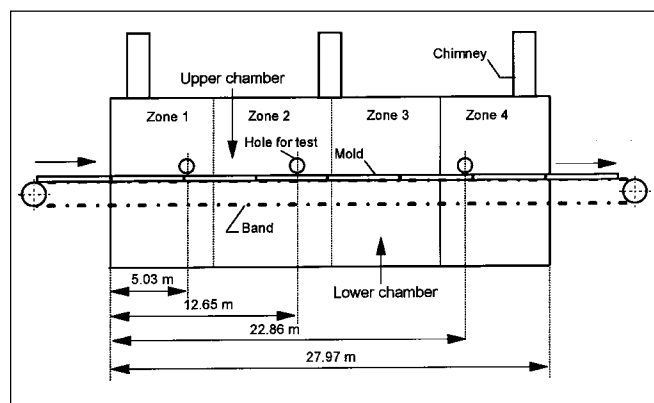


Fig. 1—Schematic of tunnel type multi-zone industrial oven.

Authors Baik and Castaigne are affiliated with the Dept. of Food Science & Nutrition, Faculty of Food & Agricultural Science, Laval Univ., Quebec City, QC, Canada G1K 7P4. Authors Grabowski, Trigui, and Marcotte are with the Food Research & Development Centre, Agriculture and Agri-Food Canada, St-Hyacinthe, QC, Canada J2S 8E3. Direct inquiries to Dr. Michèle Marcotte.

**Additional ovens.** Two additional small scale ovens were used for comparison with the industrial band oven. An electric rotary oven (MT-4-8, Équipement de Boulangerie L. P. Inc., Victoriaville, QC) was used to compare and verify the temperature distribution inside the baking chamber of the industrial scale oven. The dimensions of the rotary oven were  $2.06 \text{ m} \times 1.37 \text{ m} \times 2.01 \text{ m}$ . Electric heating elements were positioned at the bottom. The h-monitor was kept on one of 6 trays positioned horizontally during baking. For the test, the oven was operated without turning the baking trays. No air movement and vapor injection were applied during the operation. The temperature inside the oven was kept at  $204^\circ\text{C}$  during the test.

Experiments were also performed with a direct fired kitchen type electric oven. The dimensions of the baking chamber of the oven were  $0.57 \text{ m} \times 0.45 \text{ m} \times 0.4 \text{ m}$ , and the heating elements were positioned at the bottom and top. To measure the temperature gradient, thermocouples were positioned 10, 60, 110 and 160 mm below the upper heating element. No additional forced air or vapor was introduced during the operation. The operating temperature was  $204^\circ\text{C}$ .

### Absolute humidity

In order to determine the effect of vapor in the baking chamber on heat flux and effective surface heat transfer coefficient, absolute humidity was measured. A dew point meter (Hycal CT-841, Honeywell Ltd., North York, ON) was used to measure the dew point temperature of the air inside the baking chamber of the industrial oven. From dew point temperatures, the absolute humidity was then estimated using humidity calculation software, (*Humicalc*® Version 1.21w, Thunder Scientific Co., Albuquerque, NM).

### Air velocity

A thermal mass flow-meter (Series 505, Kurtz Instruments Inc., Monterey, CA) was used to measure the air velocity inside the baking chamber. A wind tunnel was built and used to calibrate and determine the relationship between the output signal in voltage and the actual air velocity from a certified mass flow-meter (LCA 6000, Chevrier Instrument Inc., Montreal, QC).

The dew point-meter and the mass flow-meter were connected to a data acquisition system, (Hydra 2520, Fluke Corporation, Everett, WA) and a portable computer. At the beginning of each test, both devices were allowed to equilibrate for 15 min inside the oven. Then, data were simultaneously collected at 1 min intervals.

### Surface heat flux and effective surface heat transfer coefficient

During baking, the convective heat flux from hot air ( $Q_c$ ) and radiative heat flux from oven interior walls ( $Q_{rw}$ ) and electric heating elements ( $Q_{re}$ ) were determined as the total top-surface heat flux ( $Q_t$ ).

$$Q_t = Q_c + Q_{rw} + Q_{re} \quad (1)$$

The convective heat flux from the hot air to the surface of the product or the plate of the h-monitor was defined as:

$$Q_c = h_c(T_a - T_s) \quad (2)$$

where,  $T_a$  and  $T_s$  are the temperatures of the air mass and surface, respectively. To include radiation in a thermal network involving convection and conduction (not considered in our case), it is often convenient to define a unit thermal radiative conductance, or radiative heat transfer coefficient as  $h_{rw} = F_{w-s} [\sigma (T_w^4 - T_s^4)/(T_a - T_s)]$ ,  $h_{re} = F_{e-s} [\sigma (T_e^4 - T_s^4)/(T_a - T_s)]$ , even if the air temperature is not the same as the wall or heating element temperature (Kreith, 1973).

Thus, radiative heat flux from the hot wall ( $Q_{rw}$ ) and heating elements ( $Q_{re}$ ) can be expressed using  $T_a$  and  $T_s$ :

$$Q_{rw} = h_{rw}(T_a - T_s) \quad (3)$$

$$Q_{re} = h_{re}(T_a - T_s) \quad (4)$$

This concept is very useful when direct measurement of radiation heat transfer is not possible. This radiant heat transfer coefficient can be treated similarly to the convective heat transfer coefficient (Kreith, 1973), in which case the total surface heat flux,  $Q_t$  can be expressed as:

$$Q_t = (h_c + h_{rw} + h_{re})(T_a - T_s) = h_t (T_a - T_s) \quad (5)$$

Hence,  $h_t$  is defined as effective surface heat transfer coefficient or overall thermal conductance by adding all heat transfer coefficients.

To measure the total surface heat flux  $Q_t$ , a commercial h-monitor and a moving temperature recorder, SMOLE (Super Multi-channel Occurrent Logger Evaluator; Electronic Controls Design Inc., Milwaukee, OR), equipped with K-type thermocouples were used. The h-monitor had aluminum target plates with emissivity similar to that of the cake (0.90–0.95), chemically anodized surfaces, to serve as a heat sink. The mass ( $m$ ), specific heat ( $C_p$ ), and surface area ( $A$ ) of the aluminum plates of the h-monitor were known. By measuring the temperature for both the air and the plate at selected intervals during the process, the total heat flux and effective surface heat transfer coefficient could be determined as a function of time.

Since Bi number of the aluminum plate of the h-monitor was  $<0.02$ , the recorded temperature at the plate center could be equated with the surface temperature. Thus, from the energy balance the effective surface heat transfer coefficient could be calculated as:

$$h_t = mC_p \Delta T / [A(T_a - T_s) \Delta t] \quad (6)$$

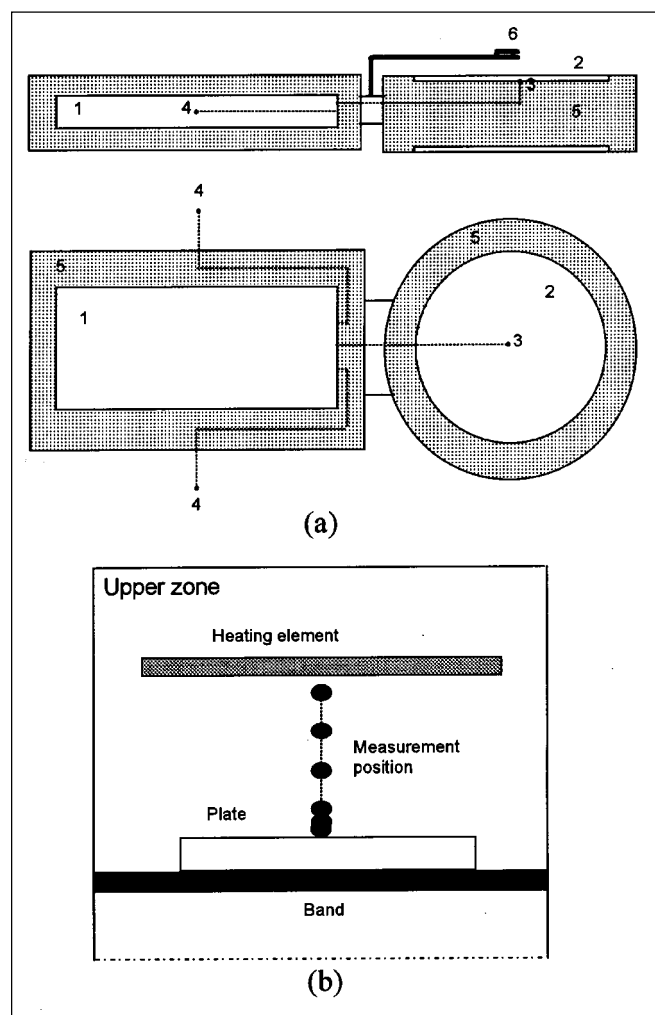


**Fig. 2—(a) Simplified description of h-monitor and (b) measurement position inside the baking chamber of the tunnel type multi-zone industrial oven. (1) SMOLE, (2) Aluminum plate, (3) Thermocouple for plate temperature, (4) The original (manufacturer) thermocouple position for air-mass temperature, (5) Insulation, (6) Thermocouple holder for air temperature measurement.**

The temperatures of the target plate ( $T$ ), and the air ( $T_a$ ), changed during the time interval, ( $\Delta t$ ); thus, it was most accurate to use relatively short time periods for calculating  $h$ -values. The manufacturer of the  $h$ -monitor, however, suggested that, for better resolution, the time period ( $\Delta t$ ) should be kept long enough to achieve a target plate temperature change ( $\Delta T$ ) of  $\geq 11.1^\circ\text{C}$ .

### Thermal boundary layer

The thermal boundary layer on the plate may be considered as an insulating layer which resists heat flow between the air mass and the plate surface of the  $h$ -monitor. This boundary layer has different properties and a different velocity from main fluid mass (Toledo, 1991). Since the convective heat transfer coefficient was defined based on air mass temperature outside the boundary layer, in order to calculate the heat transfer coefficient, the air temperature outside the thermal boundary layer should be known. In the commercial  $h$ -monitor, thermocouples for air temperature measurement were permanently centered between plates, about 20 cm from the plate horizontally (Fig. 2). To be sure that the temperature measurement of the air stream was taken out of the boundary layer, several trial measurements at different heights from the  $h$ -monitor surface were performed. Thermocouples were positioned at various heights above the center of the top plate of the  $h$ -monitor inside the baking oven (Fig. 2).

### Separation of convective and radiative heat flux

Three correlation equations were used to separate convective heat flux from total surface heat flux. From correlation equations (Eq 7–9), convective heat transfer coefficients were estimated. Radiation heat flux was then determined by subtracting the convective heat flux from total

surface heat flux. The first equation of convective heat transfer correlation for the laminar flow heat transfer to flat plate (McCabe et al., 1985) is:

$$\text{Nu} = 0.664\text{Re}^{1/2}\text{Pr}^{1/3} \quad (\text{Re} < 5 \times 10^5) \quad (7)$$

The second equation was based on an equivalent diameter approach used for a pilot scale conveyor biscuit oven (Fahloul et al., 1995).

The equivalent diameter was calculated as,  $D_{\text{eq}} = 2bH/(b + H)$ , where,  $b$  is the width and  $H$  is the height of the baking chamber, and  $\text{Re} = \text{VD}_{\text{eq}}/\nu$ :

$$\text{Nu} = 0.7\text{Re}^{0.61} \quad (\text{Re} > 40) \quad (8)$$

The third equation was the practical correlation applied for cooling and heating by the air flow over flat surfaces (Earle, 1983):

$$h_c = 5.7 + 3.9V \quad (V < 0.5 \text{ m/s}) \quad (9)$$

A prediction equation for natural convection was used as well, since the air velocity range in the industrial oven was quite low, sometimes falling between the ranges of mixed forced and natural convection (Kreith, 1973):

$$\text{Nu} = 0.82(\text{Gr Pr})^{1/5}\text{Pr}^{0.034} \quad (10)$$

When the heat transfer coefficients estimated for forced convection were lower than those for natural convection, the natural convection values were used, as had been recommended (Kreith, 1973).

### Data analysis

Each experiment was performed in triplicate. To study the effects of temperature, air velocity and absolute humidity on total surface heat flux and surface heat transfer coefficients, a statistical analysis was conducted using Software (SAS Institute Inc., 1988). Based on these results, a regression model was developed for further prediction of the effective surface heat transfer coefficient for baking conditions in a tunnel type multi-zone oven.

## RESULTS & DISCUSSION

### Baking conditions in the industrial oven

**Absolute humidity.** Absolute air humidity results at certain locations in the oven were measured (Table 1).

In the case of process A, the air humidity at the beginning of baking (0.0403 kg  $\text{H}_2\text{O}/\text{kg}$  dry air) was higher than those for the remainder of the baking process (0.0267 and 0.0276 kg  $\text{H}_2\text{O}/\text{kg}$  dry air). For process B, air humidity of the end of baking (0.0428 kg  $\text{H}_2\text{O}/\text{kg}$  dry air) was higher than those for the remainder of the baking process (0.0355 and 0.0390 kg  $\text{H}_2\text{O}/\text{kg}$  dry air). For the cake A and B baking, initial moisture of the batters was  $33.2 \pm 0.21$  and  $32.5 \pm 0.38\%$  (wet basis), and final moisture of baked cakes was  $23.73 \pm 0.50$  and  $23.1 \pm 0.55\%$ , with batter deposit rates of 10.35 and 11.28 kg/min, respectively. The humidity was from the continuous evaporation of water from the product into the baking chamber and was influenced by the setting of chimney openings in the oven. These values were lower than those for bread baking, which are reported to be between 0.29 and 1.56 kg  $\text{H}_2\text{O}/\text{kg}$  dry air (Stear, 1990). No steam injection was

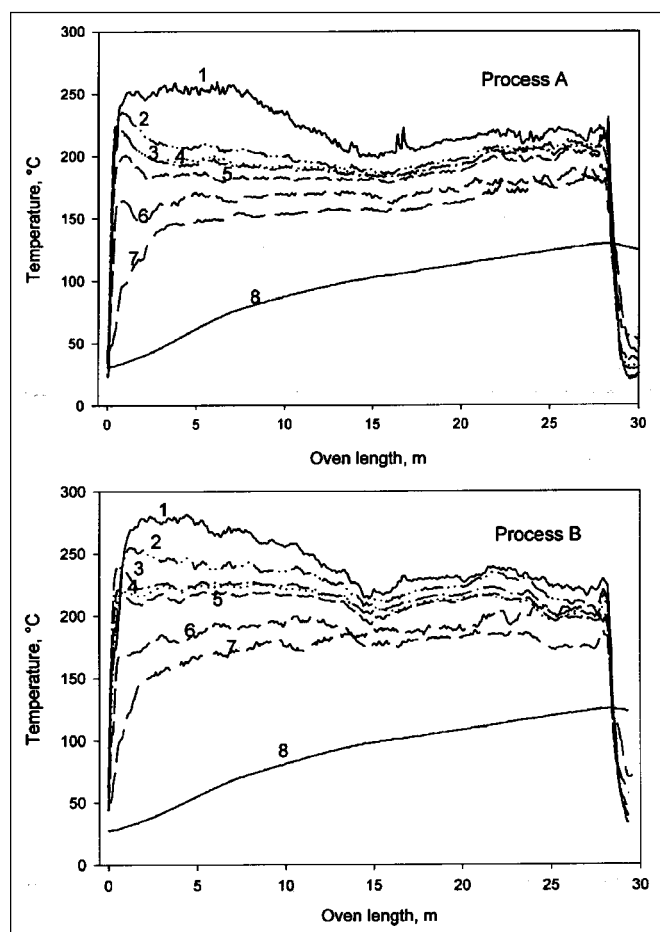


**Fig. 3—Temperature profiles of air over the plate of  $h$ -monitor during baking of cakes A and B. [(1) 190 mm over  $h$ -monitor plate for cake A and 180 mm for cake B, (2) 100 mm, (3) 50 mm, (4) 40 mm, (5) 25 mm, (6) 5 mm, (7) Original position from manufacturer, (8)  $h$ -monitor plate surface.]**

**Table 1—Absolute air humidity at baking times defined by the position of inspection holes in the industrial oven (kg  $\text{H}_2\text{O}/\text{kg}$  dry air)**

Distance from oven entrance, m	Process A		Process B	
	Baking time, s	Abs. humidity	Baking time, s	Abs. humidity
5.03	93	0.0403 $\pm$ 0.0050	70	0.0355 $\pm$ 0.0023
12.65	233	0.0267 $\pm$ 0.0047	175	0.0390 $\pm$ 0.0039
22.86	422	0.0276 $\pm$ 0.0080	316	0.0428 $\pm$ 0.0072

applied in the cake baking process unlike bread baking.

**Air velocity.** Relative air velocities strongly influence heat transfer between solid surface and gas. Since batter moves with the band, the band speed should be added or subtracted (depending on direction of the air stream) from air velocities measured at fixed position. Measured and relative air velocities were listed (Table 2) with certain locations and baking times. For both baking processes (cake A and B), relative air velocities at the beginning of baking were highest (0.39 and 0.437 m/s, respectively); then, as baking proceeded, they decreased to 0.02 and 0.062 m/s, respectively. Compare to other forced convective ovens, the magnitudes of the range of values were lower. This resulted mainly from the specific settings of ventilation speed and chimney openings optimized for cakes A and B.

**Thermal boundary layer.** The temperature distribution was determined (Fig. 3) over the aluminum plate during the baking of cakes A and B. The distance from plate to heating element was about 200 mm. A temperature gradient was observed between the heating element and aluminum plate. For cake A, temperature profiles at 40 mm and 50 mm vertically from the plate were similar. In case of cake B, at the beginning of baking temperature profiles of 40 mm and 50 mm over the plate were similar, but half way through the baking time, the temperature profile at 40 mm nearly overlapped that at 25 mm.

The temperature distributions at three positions along the baking oven were compared (Fig. 4) for cakes A and B. The shape of all profiles can be used to determine the thickness of the boundary layer and the temperature outside the boundary layer. It appeared that a

boundary layer of  $\approx 50$  mm could be estimated. The air temperature above boundary layer rose continuously toward the heating elements (Fig. 4).

In order to verify these findings in the industrial oven, a similar test was carried out in a pilot scale rotary oven. In this oven, a boundary layer was detected more clearly (Fig. 5), and its thickness was estimated to be  $< 50$  mm. Unlike the industrial band oven, no temperature gradient was observed above the boundary layer up to 200 mm from the plate of the h-monitor. In the industrial oven, the temperature gradient over the boundary layer was caused by heat transfer from the top heating elements to the layer of air flowing below it. To further corroborate that observation, the temperature distribution inside the baking chamber was measured in a direct fired kitchen type electric oven with heating elements at the top. The target oven temperature was kept at  $204^\circ\text{C}$ , while temperatures of 10, 60, 110 and 160 mm below the heating element were  $294 \pm 1$ ,  $258 \pm 2$ ,  $237 \pm 2$ , and  $218 \pm 6^\circ\text{C}$ , respectively. This distribution was very similar to that observed in the industrial band oven. Two convective heat transfer steps were observed (Fig. 4 and 5): first, diffusion from the heating element to the air-mass stream and second, diffusion through the boundary layer to the cake or h-monitor plate surface.

The selection of the proper air-mass temperature is critical for calculating convective heat transfer. The temperature at the top of the boundary layer was the input for this calculation. Temperature profiles measured at typical positions suggested by the h-monitor manufacturer were  $30^\circ\text{C}$  to  $60^\circ\text{C}$  lower than the air-mass temperature outside the

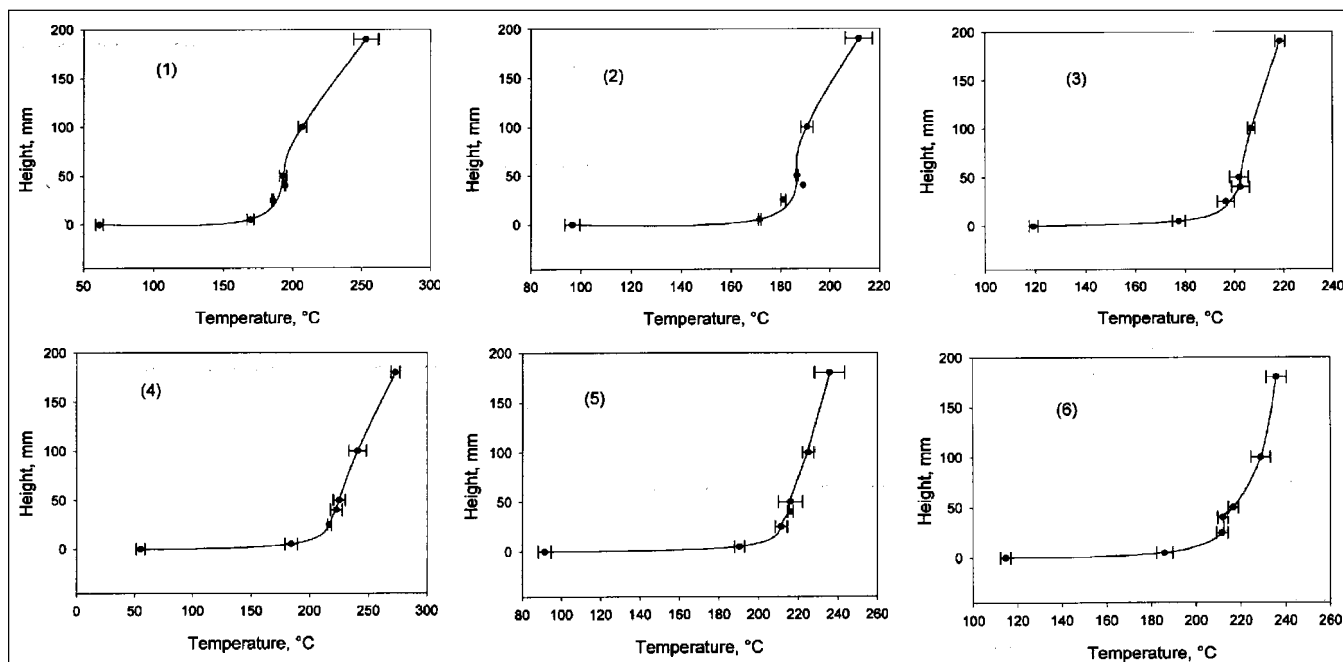


Fig. 4—Temperature distributions over the aluminum plate of h-monitor during the baking of cake A and B. [Cake A: (1) 5.03 m from the oven entrance, (2) 12.65m, (3) 22.86m; Cake B: (4) 4.7m, (5) 12.65m, (6) 22.86m.]

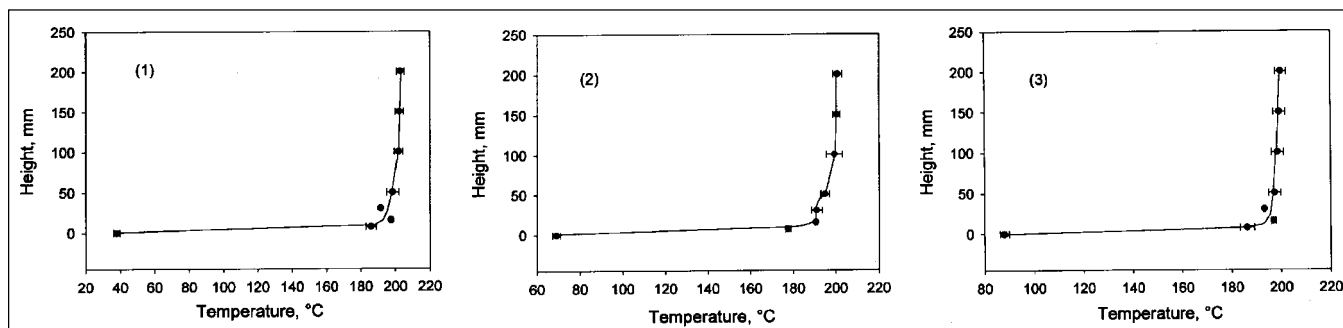


Fig. 5—Temperature distributions over the aluminum plate of h-monitor in a rotary oven after specific time: (1) 100s, (2) 330s, (3) 440s.

**Table 2—Air velocity at baking times defined by the position of inspection holes in the industrial oven (m/s)**

Distance from the oven entrance, m	Baking time, s	Process A		Baking time, s	Process B	
		Measured air velocity	Relative air velocity <sup>a</sup>		Measured air velocity	Relative air velocity <sup>a</sup>
5.03	93	0.336 <sup>b</sup> ±0.061	0.390	70	0.365 <sup>b</sup> ±0.065	0.437
12.65	233	0.065 <sup>b</sup> ±0.032	0.119	175	0.122 <sup>b</sup> ±0.098	0.194
22.86	422	0.034±0.023	0.020	316	0.314±0.048	0.062

<sup>a</sup>Corrected value by adding effect of band moving speed on measured values. Band moving speeds for process A and B were 0.0542 and 0.0723m/s, respectively.

<sup>b</sup>Air velocity values which flow in opposite direction of band moving.

boundary layer. The temperature difference of 30°C to 60°C overestimated the effective surface heat transfer coefficient by 50 to 60%. This magnitude of difference could not be neglected, even for an industrial situation. Thus, when measuring effective heat transfer coefficients by heat flux-meter, estimating boundary layer thickness is highly recommended to measure the temperature properly outside this layer.

**Heat flux and surface heat transfer coefficient.** Under constant baking condition in experimental ovens, the heat flux has been reported to be either constant (De Vries et al., 1994) or slightly decreased from 1.2 kW/m<sup>2</sup> to 0.9 kW/m<sup>2</sup> (Krist-Spit and Sluimer, 1987). In our rotary oven kept at a constant temperature of 226°C or 288°C, the surface heat flux increased slightly, then decreased slightly within the range 2244±166 and 4475±273 W/m<sup>2</sup>, respectively. For the industrial oven (Fig. 6), large differences in heat flux were observed. During baking, temperature profile, air velocity and air humidity varied substantially along the oven. A correlation between air conditions and variation of heat flux was considered, based on the statistical results. For cake A, at the beginning of the process (until 3.8 m from the oven entrance; baking time 70s), surface heat flux increased to around 6300 W/m<sup>2</sup>, then decreased quickly to 2500 W/m<sup>2</sup> at 10m (185 s), then

decreased slowly to 1503 W/m<sup>2</sup> at the end of baking.

In case of the cake B, the heat flux increased to 7550 W/m<sup>2</sup> at 4 m (55 s), decreased smoothly to 1570 W/m<sup>2</sup> at 19 m (263 s) and then increased slightly to 1950 W/m<sup>2</sup> by the end of baking. These values were much higher than the 1.7 kW/m<sup>2</sup> to 2 kW/m<sup>2</sup> measured in the indirect tunnel-type biscuit oven, operated at 200°C with 1 to 3 m/s air velocity (Fahloul et al., 1995) or 1.2 to 0.9 kW/m<sup>2</sup> for the indirect fired experimental oven kept at 220°C with 0.6 m/s (when steam injected 1.8 kW/m<sup>2</sup>) (Krist-Spit and Sluimer, 1987). In case of a direct fired experimental oven kept at 300°C without forced convection and with air flow of 1 m/s, total heat fluxes of 8 and 19 kW/m<sup>2</sup>, respectively have been reported (De Vries et al., 1994).

During the cake A baking, the ratio of radiative heat flux to total surface heat flux was from 76.1 to 80.5%. In case of cake B baking, this ratio was from 74.1 to 79.5%. Fahloul et al. (1995) reported that radiation heat transfer was 47.7 to 61.8% of total heat flux in an indirect fired continuous band oven with air velocity of 1 to 3 m/s at 220°C. Krist-Spit and Sluimer (1987) reported that bread baking in an indirect oven which was kept at 250°C with no air flow, at 250°C with 0.6 m/s of air and at 220°C with 1.5 m/s of air showed 73%, 64% and 59% radiative heat flux, respectively.

Carvalho and Martins (1992) reported that in an electric direct fired oven which was kept at 200°C, radiation heat flux accounted for about 80% of total surface heat flux. This last ratio of radiation heat transfer to total was confirmed by our results. For indirect ovens, the only radiation heat came from the oven wall, but for direct ovens radiation heat came from both heating elements and the oven walls. Thus, direct ovens showed a higher ratio of radiation heat flux. In a gas oven, only a small proportion of the heat radiating from a strip burner goes directly to the product. Most heat is used to heat walls and ceiling. In the case of electric ovens, since electric radiators generally have a larger surface area, a greater proportion of radiant heat goes to the product (Almond, 1989).

The effective surface heat transfer coefficients were determined (Fig. 7) during the baking of cake A and B. Early in the baking of cake A, it increased sharply to 46 W/m<sup>2</sup>K at 4.2 m from the oven entrance (78 s), then decreased sharply to 28.3 W/m<sup>2</sup>K at 10m (185 s), then decreased smoothly to 20.4 W/m<sup>2</sup>K until the end. The average heat transfer coefficient during the baking of cake A was 27.2 W/m<sup>2</sup>K.

In case of cake B, the effective surface heat transfer coefficient increased to 46.5 W/m<sup>2</sup>K during the first 69 s of baking (5m). Then, it decreased to 21 W/m<sup>2</sup>K at 18.5m (256 s), and then increased to 25.3 W/m<sup>2</sup>K until the end. During the baking of cake B, the average effective heat transfer coefficient was 29.3 W/m<sup>2</sup>K. The differences in both cases (A and B) were caused by the air velocity and temperature.

Experimental values of effective surface heat transfer coefficients exceeded the 23.3 W/m<sup>2</sup>K reported by Li and Walker (1996) for despatch mini-bake oven, an electrically heated reel-type oven (at 177°C). The values were lower than 83.8 W/m<sup>2</sup>K for their electric fired air-jet impingement oven and the 66.4 W/m<sup>2</sup>K for a direct gas fired air impingement oven. Since, their report did not give applied temperatures and air velocity clearly, an exact comparison of our data was not possible. The high air velocity of the air jet system may cause a higher surface heat transfer coefficient. Sato et al. (1987) reported that under baking conditions of 180 to 220°C and air velocity of 0 to 1.5 m/s, total heat transfer coefficients were recorded as 12.7–36.4 W/m<sup>2</sup>K. These values were smaller than those we found for the tunnel type oven. Huang and Mittal (1995) reported that during meat ball

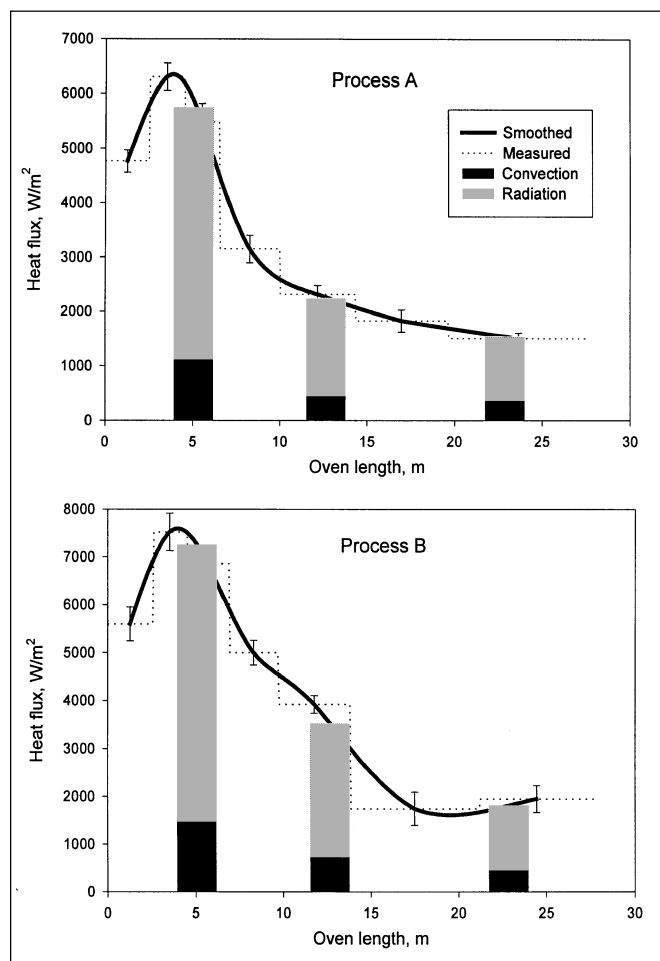


**Fig. 6—Heat fluxes during the baking of cake A and B in a tunnel type multi-zone industrial oven.**

cooking in an indirect fired commercial kitchen size oven at 140°C, varying the air velocity from 0 to 0.7 m/s, effective surface heat transfer coefficients were 9 and 23 W/m<sup>2</sup>K, respectively.

**Effect of temperature, velocity and absolute humidity of air.** A GLM procedure (SAS Institute Inc. 1988) was used to conduct a statistical analysis of the experimental data from the industrial oven, for studying the effects of temperature, air velocity and humidity on total surface heat flux and the surface heat transfer coefficient. Six levels of temperature, air velocity and humidity were randomly distributed, and each combination had a minimum of three repetitions. For the full analysis, the size, geometry and emissivity of the baking chamber and heating elements should have been included as independent variables, since they affected heat flux and heat transfer coefficients in addition to baking conditions. However, due to experimental limitations, it was not possible to analyze those parameters. The effects of temperature, velocity and humidity on the total heat flux was significant ( $p < 0.01$ ,  $p < 0.01$  and  $p < 0.05$ , respectively). An interaction of temperature and air velocity had a significant effect on total heat flux ( $p < 0.01$ ). Krist-Spit and Sluimer (1987) noted that air humidity could increase radiative heat energy, since water vapor has a higher emissivity than dry air. This was confirmed by our statistical finding of a significant air humidity effect ( $p < 0.05$ ) on the radiative heat flux ( $Q_r$ ).

Increasing the temperature and air velocity increased the effective surface heat transfer coefficient. The temperature and velocity had an effect ( $p < 0.01$ ) on surface heat transfer. An effect of air velocity on heat transfer coefficient could be clearly observed; as the air flow influenced the convective heat flux, which contributed 20–25% of

**Table 3—Linear regression model of effective surface heat transfer coefficient**

Source <sup>a</sup>	F-value	p>F	p> T	R <sup>2</sup>	SEE <sup>b</sup>	DF
$h_t = 0.0887T + 61.4V$	1388	0.01		0.993		2
$T$		0.01	0.01		0.00487	1
$V$		0.01	0.01		3.9052	1
Error						19
Uncorrected total						21

<sup>a</sup> $h_t$  is in W/m<sup>2</sup>K,  $T$  is in °C, and  $V$  is in m/s.

<sup>b</sup>SEE presents standard error of estimate.

total heat flux. The additional effect on the total heat flux could not be simply explained, since radiative heat transfer is practically independent of air movement. We inferred that air flow might affect the three-dimensional vapor layer which absorbs and emits radiative heat (Krist-Spit and Sluimer, 1987), based on the effect ( $p < 0.05$ ) of humidity and the strong influence ( $p < 0.24$ ) of humidity on radiation heat flux and the radiative heat transfer coefficient ( $h_r$ ), respectively. The effect of interactions between variables was not significant on surface heat transfer coefficients.

### Empirical prediction equation

A step-wise procedure was used for selecting variables to be included in the model. In order to select the best-fitting model, two criteria were considered, the correlation coefficient  $R^2$  and F value of the model. The prediction equation of the effective surface heat transfer coefficient was found to fit the experimental data best in the range of baking temperatures (186–225°C), relative air velocities (0.02–0.437 m/s) and humidities (0.0267–0.0428 kg H<sub>2</sub>O/kg dry air; however the humidity was not significant,  $p > 0.05$ ):

$$h_t = 0.0887T + 61.4V \quad R^2 = 0.993 \quad (11)$$

Detailed information on statistical parameters (Table 3) showed that analogous to the convective heat transfer coefficient (Eq 9), a linear effect of air velocity was observed for our effective heat transfer coefficient. Compared to the prediction model proposed by Sato et al. (1987) for an indirect electric experimental oven,  $h = 17.21V^{0.54} + 5.81 \times 10^{-2}T + 2.21$ , predicted values from our model were higher. For example at 200°C with an air velocity of 0.4 m/s, the model of Sato et al. (1987) predicted an effective heat transfer coefficient of 24.3 W/m<sup>2</sup>K, whereas our model yielded an effective heat transfer coefficient of 42.3 W/m<sup>2</sup>K. During meat ball cooking in an indirect fired kitchen oven, effective surface heat transfer coefficients 9 and 23 W/m<sup>2</sup>K were found at 140°C at air velocity of 0 and 0.7 m/s, respectively (Huang and Mittal, 1995). When these conditions were applied to our model, heat transfer coefficients of 12.4 W/m<sup>2</sup>K and 55.4 W/m<sup>2</sup>K respectively were obtained. Compared to the surface heat transfer coefficients of indirect fired ovens, those of direct fired ovens seemed higher.

According to statistical analysis, the heat transfer coefficient was affected by baking conditions, temperature and air velocity, but not by humidity. Moreover, the size, geometry and emissivity of the baking chamber and heating elements would influence this parameter. Thus, the results could only be useful for estimation of heat transfer from air to the top surface of the products for similar types of ovens. For greater accuracy, the heat transfer properties should be measured in each individual case.

### CONCLUSION

HEAT FLUX AND EFFECTIVE SURFACE HEAT TRANSFER COEFFICIENTS were measured using an h-monitor under real industrial cake baking conditions in a tunnel type multi-zone oven. Measured effective surface heat transfer coefficients combined radiative and convective conductance. In measuring effective surface heat transfer coefficients in the oven, the need to evaluate air-mass temperature was recognized and determined. Effective surface heat transfer coefficients could be used for mathematical simulations of heat and mass transfer in cake baking in a direct electric fired tunnel type multi-zone industrial oven.

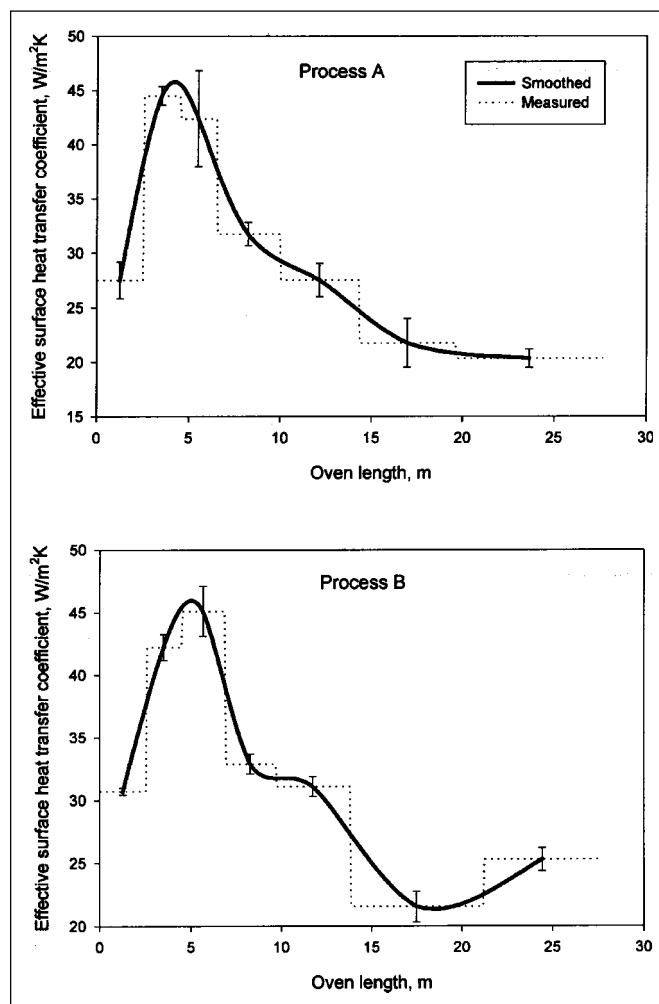


**Fig. 7—Effective surface heat transfer coefficients during the baking of cakes A and B in a tunnel type multi-zone industrial oven.**

## NOMENCLATURE

A	Area (m <sup>2</sup> )
b, H	Width and height of baking chamber, respectively (m)
C <sub>p</sub>	Specific heat (J/kg K)
D <sub>eq</sub>	Equivalent diameter of baking chamber (m)
F <sub>e-s</sub>	Radiation shape factors between heating element and product surface
F <sub>w-s</sub>	Radiation shape factors between wall and product surface
h	Heat transfer coefficient (W/m <sup>2</sup> )
h <sub>c</sub>	Convective heat transfer coefficient (W/m <sup>2</sup> K)
h <sub>r</sub>	Radiative heat transfer coefficient (W/m <sup>2</sup> K)
h <sub>re</sub>	Radiative heat transfer coefficient between heating element and product surface (W/m <sup>2</sup> K)
h <sub>rw</sub>	Radiative heat transfer coefficient between inner wall and product surface (W/m <sup>2</sup> K)
h <sub>t</sub>	Effective surface heat transfer coefficient (W/m <sup>2</sup> K)
m	Mass (kg)
Q <sub>c</sub>	Convective heat flux (W/m <sup>2</sup> )
Q <sub>re</sub>	Radiative heat flux from heating element (W/m <sup>2</sup> )
Q <sub>rw</sub>	Radiative heat flux from inner wall of oven (W/m <sup>2</sup> )
Q <sub>t</sub>	Total surface heat flux (W/m <sup>2</sup> )
T	Temperature (°C)
Δt	Time period (s)
V	Fluid velocity (m/s)
ν	Kinematic viscosity (m <sup>2</sup> /s)
σ	Stephan Boltzman constant, $5.67 \times 10^{-8} \text{W/m}^2\text{K}^4$

## Dimensionless numbers

Gr	Grashof number
Nu	Nusselt number
Pr	Prandtl number
Re	Reynolds number

## Subscripts

a	Air
c	Convection
rw	Radiation from inner walls
re	Radiation from heating elements
s	Surface
t	Total

## REFERENCES

- Almond, N. 1989. *Biscuits, Cookies, and Crackers*. Vol. 2. Elsevier Applied Science, London/New York.
- Baik, O. D., Sablani, S. S., Marcotte, M. and Castaigne, F. 1999. Modeling the thermal properties of a cup cake during baking. *J. Food Sci.*: In press.
- Booth, R. G. 1990. *Snack Food*. Van Nostrand Reinhold, New York.
- Carvalho, M. G. and Martines, N. 1992. Mathematical modeling of heat and mass transfer in a forced convection baking oven. In *AIChE Symposium Series-Heat Transfer*, San Diego, CA, p. 205-211.
- De Vries, U., Velthuis, H. and Koster, K. 1994. Baking ovens and product quality-a computer model. *Food Sci. Tech. Today*. 9: 232-234.
- Earle, R. L. 1983. *Unit Operations in Food Processing*. 2nd ed. Pergamon Press, Ltd., Oxford.
- Fahloul, D., Trystram, G., Duquenoy, A. and Barbotteau, I. 1994. Modelling heat and mass transfer in band oven biscuit baking. *Lebensm. Wiss. Technol.* 24: 119-124.
- Fahloul, D., Trystram, G., McFarlane, I. and Duquenoy, A. 1995. Measurements and predictive modelling of heat fluxes in continuous baking ovens, *J. Food Eng.* 26: 469-479.
- Huang, E. and Mittal, G. S. 1995. Meatball cooking-modelling and simulation. *J. Food Eng.* 24: 87-100.
- Kreith, F. 1973. *Principles of Heat Transfer*. 3rd ed. Intext Educational Publishers, New York/London.
- Krist-Spit, C.E. and Sluimer, P. 1987. Heat transfer in ovens during the baking of bread. In: *Cereals in a European Context*, 1st European Conference on Food Sci. & Tech. Morton, I. D. (Ed.), p. 346-354. Ellis Horwood publishers, Chichester, UK.
- Li, A. and Walker, C.E. 1996. Cake baking in conventional, impingement and hybrid ovens. *J. Food Sci.* 61: 188-191.
- McCabe, W.L., Smith, J.C. and Harriott, P. 1985. *Unit Operations of Chemical Engineering*. 4th ed. McGraw-Hill Book Co., New York.
- Özilgen, S. and Heil, J.R. 1994. Mathematical modelling of heat and mass transport in a baking biscuit. *J. Food Process Preserv.* 18: 133-148.
- Sablani, S.S., Marcotte, M., Baik, O.D. and Castaigne, F. 1998. Modeling of simultaneous heat and water transport in the baking process: A review. *Lebensm. Wiss. Technol.* 31: 201-209.
- SAS Institute, Inc. 1988. *PC-SAS® User's Guide, Edition 6.03*, SAS Institute, Inc., Cary, NC.
- Sato, H., Matsumura, T. and Shibukawa, S. 1987. Apparent heat transfer in a forced convection oven and properties of baked food. *J. Food Sci.* 52: 185-188, 193.
- Savoie, I., Trystram, G., Duquenoy, A., Brunet, P. and Marchin, F. 1992. Heat and mass transfer dynamic modeling of an indirect biscuit baking tunnel oven. Part 1. Modeling principles. *J. Food Eng.* 16: 173-196.
- Sluimer, P. and Krist-Spit, C.E. 1987. Heat transfer in ovens during the baking of bread. In: *Cereals in a European Context*, 1st European Conference on Food Sci. Tech. Morton, I. D. (Ed.), p. 355-363. Ellis Horwood publishers, Chichester, UK.
- Stear, C.A. 1990. *Handbook of Bread Making Technology*. Elsevier Applied Science, London/New York.
- Toledo, R.T. 1991. *Fundamentals of Food Process Engineering*. 2nd ed. Van Nostrand Reinhold, New York.
- Zanoni, B., Pierucci, S. and Peri, C. 1994. Study of the bread baking process-II. Mathematical modelling. *J. Food Eng.* 23: 321-336.

Ms received 10/2/98; revised 3/3/99; accepted 3/6/99.